GATM: A 3-D FE Fusion Magnet Model and Application to DIII-D and Next-Generation Devices

James A. Leuer, *Member, IEEE*, D. Weisberg, R. MacDonald, I. Favela, Paul Beharrell,
D. Appelt, R. Buttery, C. Crowe, N. Eidietis, B. Grierson, L. Holland, K. Holtrop,
A. Kellman, James L. Luxon, C. Murphy, Z. Piec, G. Sips, *Member, IEEE*,
M. Van Zeeland, and Amani Zalzali

Abstract— The General Atomics Tokamak Model (GATM) is a recently developed finite element (FE) environment for assessing the performance of tokamak magnet-plasma systems. Its generic environment is designed to assess magnet performance parameters for existing tokamaks, such as Doublet-III-D (DIII-D) and next-generation tokamak. GATM's environment consists of a number of models, including a Comsol 3-D FE model and routines connecting this model to other GA tools. GATM consists of a 2-D axisymmetric module characterizing Poloidal Fields (PFs) system magnetic properties, including an equilibrium fitting code (EFIT) plasma representation. The 2-D module contains a central solenoid (CS) structural model for stress and deflection assessment. Toroidal field (TF) coils are characterized by a 3-D magnetics module for TF calculations and simulation of TF nonaxisymmetric ripple. PF and TF magnetics models provide input to a 3-D TF structural module, which simulates both in-plane and out-of-plane stress. A 3-D TF center post module uses input from the other three modules to evaluate the performance of a superconducting coil including details of the case, winding-pack, and superconducting cable. Model geometry, (Plasma, TF, CS, PF, and structures) is fully parametrized and allows for rapid assessment of arbitrary tokamak configurations. The GATM model is under development and is intended to interface with other general atomics models including: GA System Code (GASC), dynamic tokamak system model (TokSys), recently developed FUsion Synthesis Engine (FUSE), and DIII-D database, including EFIT. Models and current states generated in the GATM environment are output to engineering relevant codes ANSYS and SolidWorks. The article provides an overview of the present GATM environment and its application to DIII-D's TF coil and an advanced tokamak (AT) Fusion Pilot Plant (FPP).

Index Terms— Comsol, doublet-III-D (DIII-D), exhaust and confinement integrated tokamak experiment (EXCITE), finite element (FE), fusion, fusion pilot plant (FPP), magnet, plasma, poloidal coil, superconductor, system studies, tokamak, toroidal coil.

NOMENCLATURE

a	Minor radius.
B_0	Toroidal magnetic vacuum field ($@ R_0$).
C_{Ejima}	Plasma resistive loss coefficient [11].
I_p	Plasma current.
J_p	Plasma current density.
R_0	Major radius.
R_{CP}	Center post midplane central radius.
$\mathfrak{R}_p$	Plasma loop resistance.
R_{TF}	TF central radius of max Z (ellipse boundaries).
$R_{\text{TF\_leg}}$	Outer TF *leg* center radius.
Z_{CP}	Center post height.
ΔR_{CP}	Center post midplane build.
$\Delta R_{\text{CP\_CS}}$	Gap between center post and central solenoid.
ΔR_{CS}	Center Solenoid midplane build.
δ	Triangularity.
θ	Poloidal angle parameter ($-\pi \leq \theta > \pi$).
κ	Elongation.
μ_0	Permeability of free space.
ξ	Squareness.
ρ	Plasma toroidal resistivity.
Φ	Poloidal flux.

Subscripts:

CP	Center post (TF), also referred to as central column.
CS	Central solenoid (PF).
I	Inductive.
IM	Initial Magnetization state (plasma breakdown).
p	Plasma.
PL	Plasma state (start of current flattop).
R	Resistive.
SC	Superconducting.

I. INTRODUCTION

THE General Atomics Tokamak Model (GATM) finite element (FE) code is being used to analyze DIII-D's [1] Toroidal Field (TF) coil and for analysis of potential next-step devices, such as the Exhaust and Confinement Integrated Tokamak Experiment (EXCITE) [2] and Fusion Pilot Plant (FPP) [3]. The model was developed within the Comsol Multiphysics [4] environment to provide both a fixed geometry analysis of DIII-D's coil systems and a parameter-driven model for both Poloidal Field (PF) and TF coil analysis in future devices. The latter capability provides a method for performing system studies much like the GA System Code (GASC) [5]. It is integrated into the GA tokamak analysis
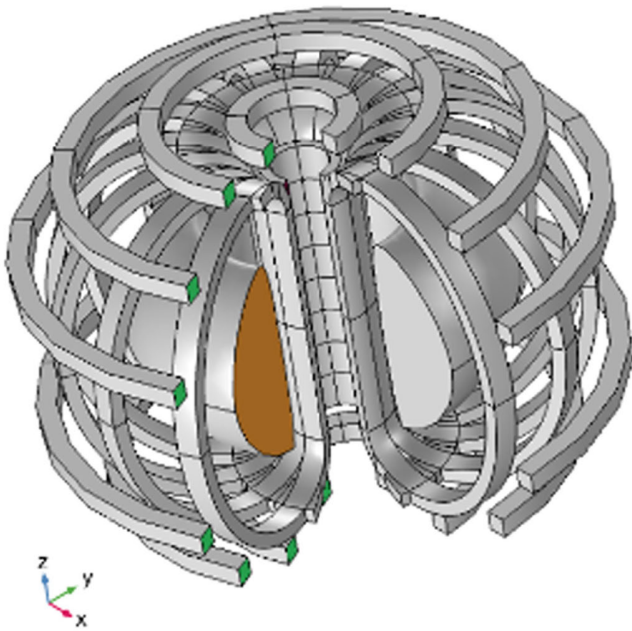
Fig. 1.   GATM's Full 3-D FE parametric model of a next-generation tokamak magnet/plasma system.
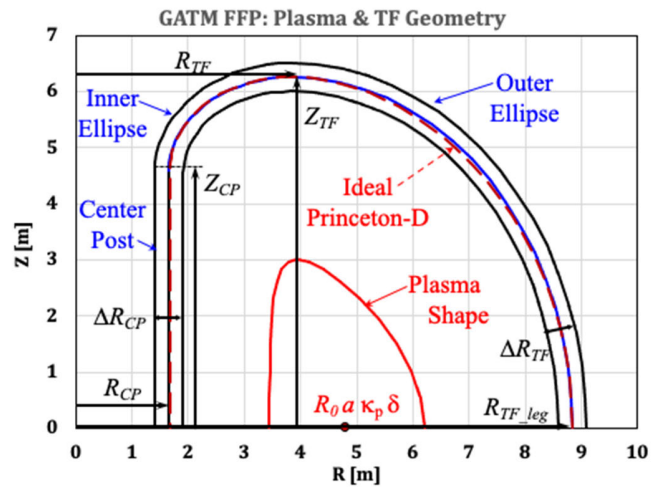

Fig. 2.   GATM input parameters for FPP design for plasma and TF coils. Also shown in the red dashed line is the ideal central contour for a bending-free Princeton-D [24] shaped TF coil with similar parameters to FPP.

framework, including GASC, FUSE[1], and TokSys [6], and is able to interface with equilibrium fitting code (EFIT) [7] and the DIII-D shot database [8]. Fig. 1 shows an example of a FPP design containing all 16 TF coils. In an actual TF magnet analysis, a single coil leg is modeled, and appropriate cyclic boundary conditions are invoked to emulate all TF coils.

The intent of this article is to initiate documentation of GATM's framework, formulas, and its application to existing and future tokamaks. Specifically, in Section II, we define the four modules that make up the GATM Comsol model. Section III covers the usage of individual models within each module for performance evaluation of Sections III-A DIII-D and III-B FPP. Section IV provides insight into the interface between GATM and other GA-developed tools and connections with commercially available structural analysis codes. Finally, Section V provides a summary and overview of continuing model development. Appendix A provides basic geometric formulas used in the models. Appendix B provides an overview of the MATLAB mapping algorithm used to scale DIII-D shot data into the GATM FE model.

II. GATM MODELING ENVIRONMENT

The GATM FE model has been developed within the Comsol Multiphysics environment. This modeling framework provides GUI-driven developmental tools, as well as low-level, equation-based access to the underlying partial differential equations (PDEs), and provides a unique, unified approach to FE analysis of physics/engineering problems. The model was developed to allow computation of magnet systems typical of a tokamak magnet configuration in both 1) a fixed geometry model (e.g., DIII-D's TF, Ohmic Heating (OH) and Field Shaping coils [1], [15]) and 2) a completely parameter driven model for system studies and connections to other GA tokamak engineering/physics tools. The basic modular framework provides input blocks that can easily be modified to simulate

other existing or future tokamak devices. Component geometry and current state input variables are separated into functional parameter nodes for ease of model development. Although only currently applied to a small number of tokamaks, future applications to other existing machines such as ITER [9] will provide some connection to extensive FE analysis in the literature and provide a pseudo-validation of the modeling environment.

The GATM FE model contains modules to emulate magnet performance with the Comsol module shown within ()'s.

1) *2-D Axisymmetric PF (ac/dc):* Includes all PF coil and plasma, geometries, and current states [7] and contains a sub-model to assess the CS structural properties.
2) *3-D Magnetics [TF Coil (ac/dc)]:* Provides TF coil self-field magnetics, including nonaxisymmetric fields like TF ripple.
3) *3-D Structural [TF Coil (Structural Mech.)]:* Uses PF and TF magnetics to determine in-plane and out-of-plane TF stresses and includes parametrized lateral support systems.
4) *3-D Structural TF CP (Struct. Mech.):* Sub-model of TF coil CP, containing a parameterized geometry to model: Case and Winding-pack structure with embedded superconducting cable.

Each module contains a geometrical and application section representing physics/engineering phenomena [4]. The magnet geometry of each module is either fixed or driven by user-input plasma/magnet parameters. Several different geometric models exist for generating the overall plasma/magnet geometry (see Appendix A). For system studies, magnet and plasma geometries are connected by formulas allowing easy manipulation of the final topology. Plasma geometry is specified by the typical tokamak shape parameterization: R_{op}, a_p, κ_p, δ_p, ξ_p [14]; an EFIT plasma equilibrium, composed of boundary shape and plasma current states, is input for more detailed studies. PF coils are located with clearance from the outer TF surface and positioned to ensure space for remote maintenance requirements. Fig. 2 shows an FPP plasma and TF with major input variables defined. The centerline of the TF coil is shown in blue. In addition, a "Princeton-D" shape [24] is shown in a red dashed line with major parameters defined by inner/outer TF midplane radii. The actual FPP TF shape is shown to

---

[1]Fusion Synthesis Engine (FUSE) is a tokamak modeling environment being developed at GA to integrate proven physics, engineering, and costing models into a self-consistent simulation and design package.
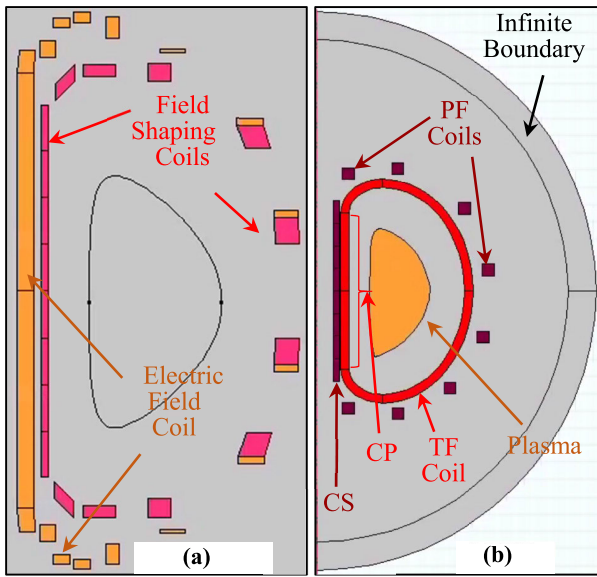
Fig. 3. Two-dimensional axisymmetric PF model. (a) Fixed geometry DIII-D E and F-coils. (b) FPP 2-D axisymmetric model containing 1) plasma mapped from a DIII-D discharge, 2) TF cross section (for reference only, not used in FE solution), 3) CS, and 4) PF coils. The exterior matching boundary is shown as the outside circular region. Note that figures A and B are not the same scale, with $R_{0\_DIII-D} = 1.67$ m and $R_{0\_FPP} = 4.82$ m.

Fig. 4. Three-dimensionl magnetics and structural models. (a) DIII-D TF coil with detail showing the finger joint geometry and steps for in-plane loading. The finger joint is composed of 13 fingers and 14 inserts [1], [15]. (b) FPP parameter generated structural model containing structural components for overturning loads. The subpanel shows details of the fourth module in GATM which contains the CP case/winding-pack/superconductor model.

closely follow the Princeton-D, which is approximately a bending-free shape.

The 2-D axisymmetric PF Module contains all elements needed to determine the PF fields in the various magnets. Fig. 3(a) shows the fixed geometry PF coil system used to approximate the E-coil (Electric field coil, also called OH coil) and 18 F-coils (Field shaping coils) in DIII-D [1], [15]. Fig. 3(b) shows the FPP computational domain for the 2-D axisymmetric model including the TF coil geometry, which is absent in the final 2-D FE analysis. In the parameterized model, the CS and outer PF coils are mapped from the outer contours of the TF coil using GASC and PF spacing requirements. The outer circular region represents the infinite domain boundary elements used to model free space.

Fig. 4 shows the TF coil geometry used in the magnetics and structural models for DIII-D and FPP. Ultimately both models are wedge-shaped domains with appropriate cyclic conditions applied to the edges. The magnetics and structural models are separate in the GATM environment (Module 2 and 3, respectively) to allow additional nonconducting structures in the stress model to react to PF overturning loads. The 2-D PF and 3-D TF magnetic models provide input fields for generating body loads in the 3-D TF structural module. The DIII-D model has much more complex geometry than the parameter-driven models, including all the details of the finger joints and additional boundary loading surfaces. The 3-D TF structural model uses a homogeneous, smeared property model over the TF cross section, while the 3-D CP model uses the material properties of each component. A fourth module is included, which contains a 3-D CP model with details of the case, winding-pack, and superconductor geometry. The CP model boundary conditions are extracted from the 3-D structural model (Module 3). This model is typically only used when more detailed stresses in the super-conducting cable are needed.

All currents in the system, PF, TF, and Plasma (PL) are input parameters. Specifically, the model contains three internal
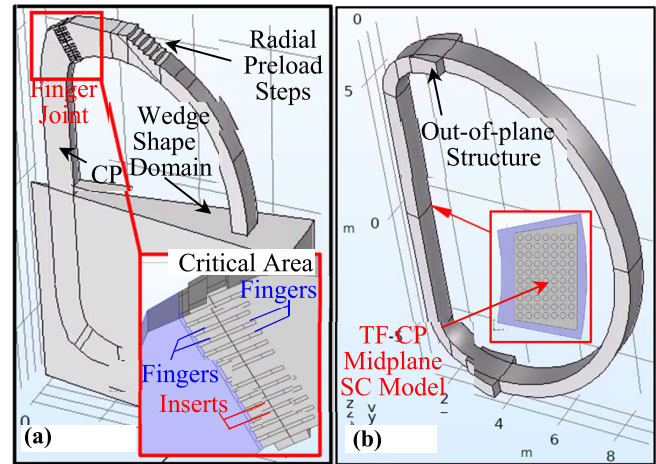
states used to quickly assess three load conditions. Typical states loaded into the system are IM state (Initial Magnetization also plasma initiation), PL state (usually defined by the end of plasma current ramp or end of discharge), and a third, off-normal state. Any arbitrary set of currents can be loaded into any state, but for scoping studies, IM and PL states are typically used for the evaluation of magnet performance. They are established based on plasma evolution modeling. In the present study, we are mapping an actual DIII-D discharge, including plasma equilibrium to establish the IM and PL states (see Appendix B). The framework is general and allows for input of other equilibrium data or model-generated states. Overall, GATM FE magnetic calculations have been validated with Biot–Savart-type models in TokSys.

III. APPLICATION TO TOKAMAKS

The model has been applied to three tokamak devices: DIII-D, EXCITE, and FPP. In this section, we focus on Section III-A fixed geometry model to simulate DIII-D and Section III-B parameter-driven model to simulate FPP. The workflow used to generate the EXCITE model is essentially identical to the FPP case.

A. Application to DIII-D

The original Doublet III (DIII) [15] device was designed in the late "70s" and was modified to the DIII-D configuration in the "80s." It has operated for over 45 years. DIII-D's TF coil (B-coil) was designed using an in-house developed 2-D FE code and quasi-2D beam SAP IV [17] model to quantify coil design limits based on stress and displacements in the DIII-D TF coil [16]. During the development of GATM, the DIII-D TF coil was considered a prime candidate for initial application and testing of the model's capability. A fixed geometry module was introduced into the GATM environment to allow for the complex system geometry and boundary conditions to be modeled. In particular, the finger joints, horizontal preload, and lateral loading systems were incorporated in the model to represent important features and boundary conditions unique to DIII-D. As with the original design study [16], we use a spring constant, K_y to represent DIII-D's lateral, out-of-plane
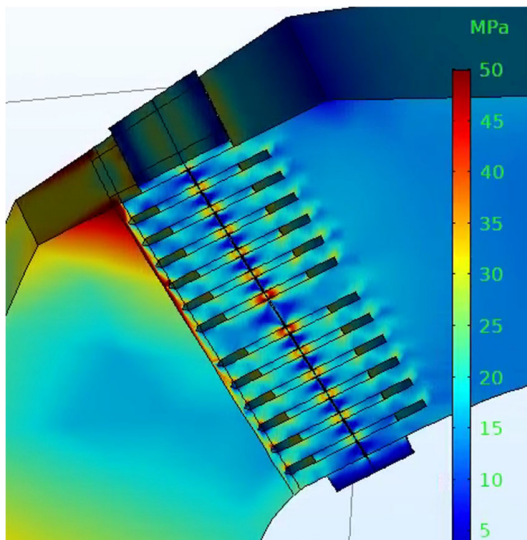
Fig. 5. DIII-D's TF CP and finger joint von Mises stress for DIII-D shot s173986 with $I_B = 127$ kA, $I_P = 1.8$ MA, $I_E = 2 \times 82 = 164$ kA, and $K_y = 90$ MN/m.

support system (Anti-Torque Frame) [1], [15]. An experimentally determined spring constant ($K_y = 90$ MN/m) is used to represent the structure rather than values published in the literature [16], [19]. In addition, load states associated with the horizontal preload system [$F_P = 0.533$ MN (120 kips)] and CP radial prestress [$P_{CP} = 8.34$ MPa (1.21 ksi)] are introduced as a base load for stress evaluation.

The main design limitations of the DIII-D TF coil are believed to be in the outer extremes of the CP close to the finger joint and the finger joints themselves (see Fig. 4). In particular, the original thick copper plates manufactured for use in CP fabrication were found to contain flaws and an effort was undertaken to extensively test and analyze the coil for fatigue design limit determination [20]. These areas were closely scrutinized in the GATM analysis, including sub-griding regions of the outermost turns (turns 1 and 6 of the six-turn domain) in the critical areas of the finger joint and its CP interface. Fig. 5 shows primary von Mises stress for a particularly high plasma current shot (s173986@3s, $B_0 = 2.2$ T ($I_{TF} = 127$ kA, DIII-D's operational limit), $I_P = 1.8$ MA) and one that has the largest predicted stresses. The figure is plotted with a reduced stress range to accentuate the high-stress regions (red); peak stresses are higher. Stress is seen to be elevated in the upper/CP and finger joint region and is commensurate with areas identified in original TF coil design documents.

In evaluating the present design limits using the GATM environment, we use the same criteria as used in the design documents [16], [18], [19], which use modified ASME criteria [21]. Design limits are determined by evaluation of 1) maximum membrane stress and 2) fatigue limit stress, defined by operational alternating stresses. Many different plasma shots were considered in the analysis; here, we show some of the maximum stress shots. The present and previous DIII-D TF analyses use linear models (smeared property and nonslip conditions) and have been shown to well represent the DIII-D TF coil structural properties [16], [17], [18], [19], [20]. With fixed out-of-plane spring constant Ky, loads from various sources can be superimposed and are used in the modeling environment to scale to different machine performance metrics.

Fig. 6 shows stress plots for three particularly energetic DIII-D discharges, with calculations of the (a) finger membrane, (b) insert membrane, (c) finger fatigue, and (d) insert fatigue, stresses. The index on the X-axis refers to the insert/joint location with numbering starting at the joint top. Also, shown in the figure are the original DIII-D design values computed using the 2-D analysis but corresponding to a much higher loading condition ($I_{TF} = 196$ kA, $I_E = 2 \times 110 = 220$ kA [16]). The applicable design limit for the component material is shown in the red line.

The GATM results show that considerable margins exist over material stress allowable when operating at DIII-D's $I_{TF} = 127$ kA operational limit. This is well known since DIII's original $I_{TF} = 195$ kA design [16] would require extensive support modification, costly power supply upgrades, and risky dynamic loading to achieve this level of performance. However, the number of "shot counts" is approaching 200 000, while the original design specified 100 000 full performance (195 kA) cycles. Over the years, CP material testing and fatigue analysis, combined with DIII-D's operational history, have established expected TF life limits [18], [19]. Combined with GATM results, we predict 66% of the CP fatigue life has been used in the TF's 45 years of operation. Assuming future operations are similar to the past, DIII-D's TF has many more years of operation. Other studies were performed using the GATM environment including thermal and CP epoxy shear stress studies. For the most part, results confirm previous simplified analysis [16], [17], [18], [19], [20] and at DIII-D's TF $I_{TF} = 127$ kA operational limit, all performance metrics have adequate safety margins.

B. Application to FPP

The main thrust of the GATM development was the creation of an environment to expedite the analysis of superconducting magnet systems for next-generation tokamaks. For many years GA has explored potential Advanced Tokamak (AT) concepts in compact tokamak devices [2], [3] for application to an AT FPP, here referred to as FPP. The optimized GASC/FUSE plasma parameters for the FPP design are as follows:

$$R_{0p} = 4.824 \text{ m} \quad a_p = 1.378 \text{ m}$$
$$\kappa_p = 2.19 \quad \delta_p = 0.7$$
$$I_p = 9 \text{ MA} \quad B_0 = 4.71.$$

In addition, GASC or FUSE CS, TF, and plasma midplane geometries are direct inputs in GATM. The GASC/FUSE FPP design is optimized for steady state, auxiliary current drive operation and, ohmic flux is used primarily for plasma current ramp-up. In the FPP GATM design, a small reduction in the CS inner radius was introduced to add extra ohmic flux for potential FPP pulsed operation. The PF coil configuration is established based on spacing requirements with the outer TF surface and remote maintenance requirements. Fig. 3(b) shows the geometry used in the study. Structural boundary conditions are introduced at the bottom of TF and CS coils. Stainless steel properties are used in the various FPP coil structural components.

GATM allows input of a detailed plasma equilibrium, while the 2-D PF magnetic model generates flux and fields required for stress analysis of various magnets. In the present study, the PF and plasma current states are mapped from a DIII-D shot (see Appendix B). One of DIII-D's early high-performance discharges (s87980) is used as an example here; any DIII-D
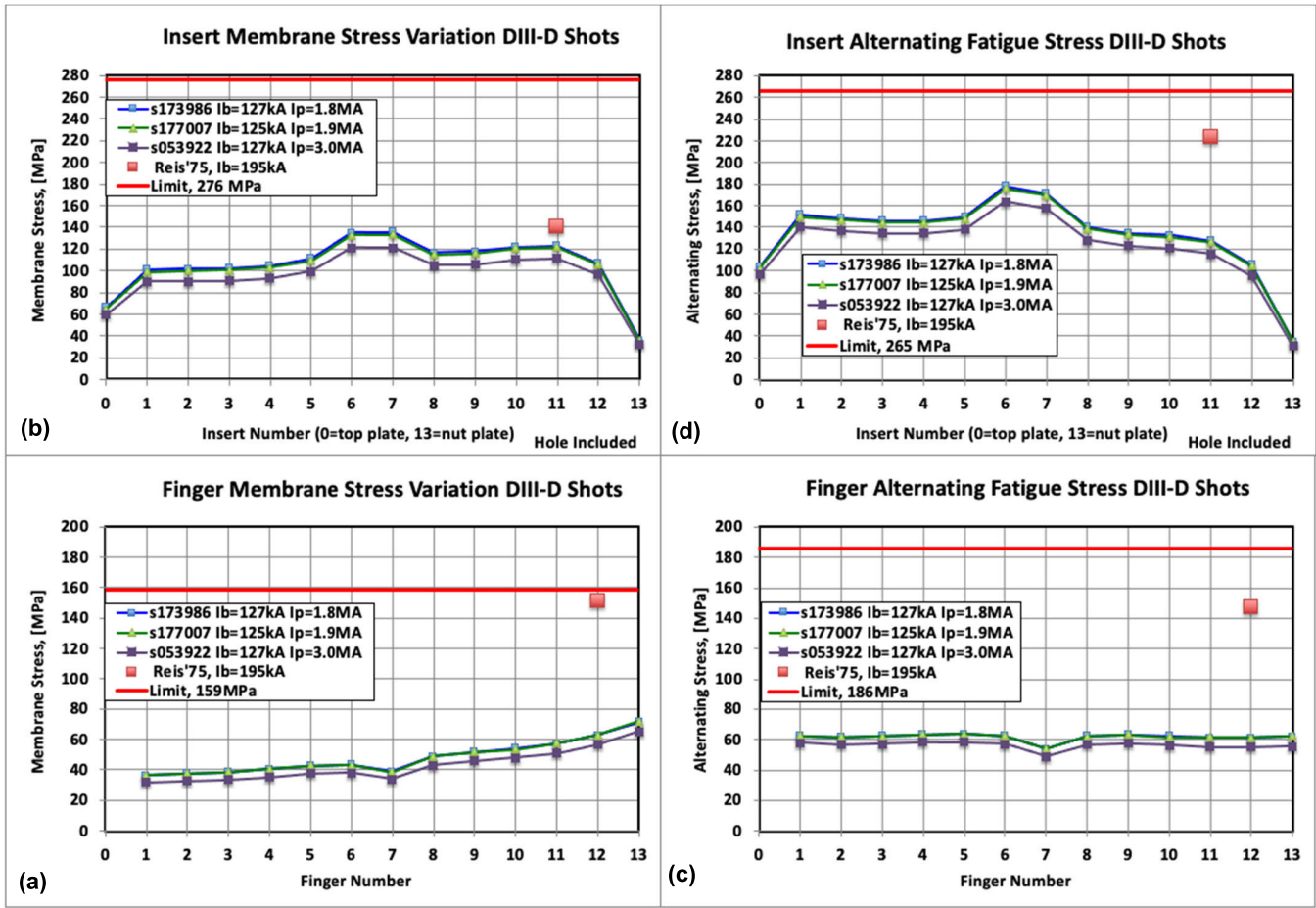
Fig. 6. Design stress parameters for select DIII-D discharges in the finger joint area. Insert and finger identification numbering on the X-axis starting at the top of the TF. Various curves contain: Selected shots, Reis/75 original component predicted stress (red square), and component material allowable stress for 100 000 cycles (red lines) [16]. (a) Finger membrane stress, (b) insert membrane stress, (c) finger fatigue stress, and (d) insert fatigue stress. X numbering is from the joint top.

shot can be evaluated in this manner. Both the IM and PL states are simulated for inclusion in the GATM model. With a steady-state device, like our steady-state AT FPP design, we use the Start-Of-Flattop (SOF) as the PL state and scale from the actual current ramp-up in DIII-D to establish the IM and PL flux to approximately produce equal peak stresses in the CS. The mapping routines allow for the correct flux partitioning between these states using the resistive flux scaling established early in DIII-D's history (usually designated the "Ejima Coefficient [11], C_{Ejima}). Fig. 7(a) shows IM state B-field contours required to establish a 34 Vs flux plateau for plasma breakdown, which typically occurs in regions of <20 G [23]. Fig. 7(b) shows the original DIII-D equilibrium flux contours extracted from the EFIT reconstruction. Fig. 7(c) shows the flux contours of the equilibrium scaled into the FPP device. Both the IM flux value, $\Phi_{\mathrm{IMo}} = 34$ Vs, and the PL boundary flux $\Phi_{\mathrm{PLx}} = 0$ Vs, were adjusted to produce approximately equal stresses in the CS using a resistive flux loss coefficient $C_{\mathrm{Ejima}} = 0.35$. Note that the PL central flux $\Phi_{\mathrm{PLo}} = 32$ Vs is slightly below the 35 Vs IM boundary flux and this is a characteristic of low resistive loss startups.

Fig. 8 shows CS coil von Mises stresses calculated based on the 2-D PF magnetics model and includes a GASC determined stress multiplier ($f_{\mathrm{CS}} = 1.14$), at (a) IM and (b) PL states. Peak stresses are reasonably balanced, with $\sigma_{\mathrm{CS\_IM}} = 140$ MPa and $\sigma_{\mathrm{CS\_PL}} = 152$ MPa, and much lower than the 800 MPa typi-
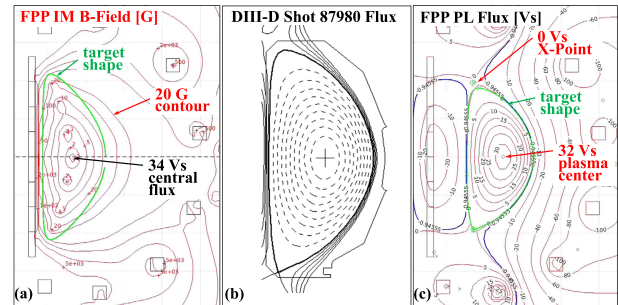

Fig. 7. (a) FPP IM state showing PF B-field contours, and some important quantities: target shape, Central Flux = 34 Vs and the 20 G B-field contour within which plasma breakdown is expected [23]. (b) Original DIII-D EFIT equilibrium flux contours for the target shot 87980. (c) FPP PL state scaled from DIII-D shot 87980, with the scaled target DIII-D shape shown in green; also shown are flux values at the plasma center = 32 Vs and plasma X-point = 0 Vs (separatrix).

cally used as GASC's magnet stress limit [2], [3]. Low values are attributed to an increased CS thickness added to the GASC baseline value to allow for a substantial Ohmic flat-top current drive. Note, that allowable stress values of 800 MPa were used for consistency with GASC's static analysis; however, when the CS cyclic nature is included reduced allowable is expected.
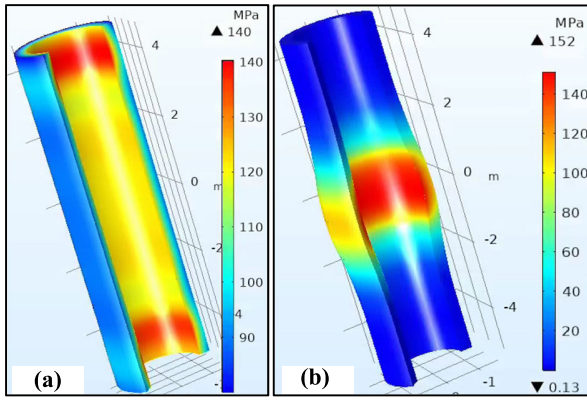
Fig. 8.   FPP CS von Mises stress for (a) IM state: $\Phi_{\mathrm{IMo}} = 34$ Vs and (b) IP state: $I_p = 9$ MA.
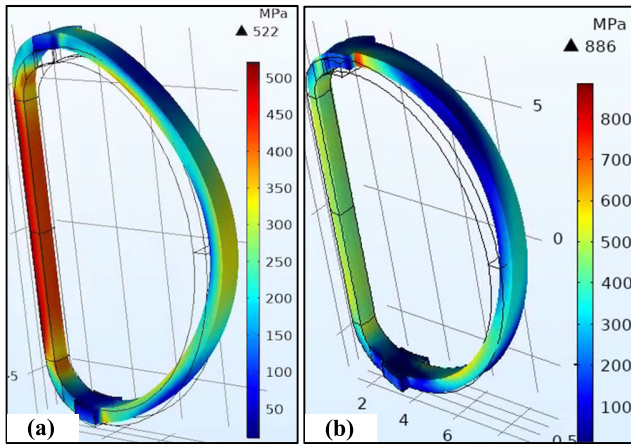

Fig. 9.   FPP TF von Mises stress for (a) IM state: $\Phi_{\mathrm{IMo}} = 34$ Vs and (b) PL state: $I_p = 9$ MA. The deflected shape reflects relative displacements from nominal geometry (black).

Fig. 10.   Detailed stress in the TF CP sub-model–von Mises stress for (a) IM state: $\Phi_{\mathrm{IMo}} = 34$ Vs and (b) PL state: $I_p = 9$ MA. (c) Shows the 3-D nature of the model for the PL stress state.

Fig. 11.   GATM's interaction with GA tokamak modeling environment and with commercial FE codes.

Fig. 9 shows the TF von Mises stresses from the 3-D TF structural model, including a GASC-determined stress multiplier $f_{\mathrm{TF}} = 1.26$, for the (a) IM and (b) PL states. Peak stresses are highest at the PL state with: $\sigma_{\mathrm{TF\_IM}} = 886$ MPa and slightly over the 800 MPa limit used in GASC. The PL peak stresses are a result of out-of-plane loads; the maximum stress is seen to be just outside the anti-torque structure. Outside TF leg lateral deflections are ∼9 cm and reduction will require outside lateral support. Subsequent mapping of the GATM-generated system into the Ansys environment (see Fig. 11) and further model development, introduced additional outside structures which reduce TF peak stresses and outside TF leg lateral deflections. The midplane stress is seen to be ∼500 MPa and similar to the peak stress in the IM state $\sigma_{\mathrm{TF\_IM}}$ = 522 MPa. This is as expected since the IM state produces a constant flux plateau in the plasma region and the poloidal flux approximately follows the TF current flow, resulting in low out-of-plane bending loads. Essentially, the IM state is close to the in-plane stress state of the TF-only current.

The 3-D CP structural model results are shown in Fig. 10. Details of the midplane SC cross section can be seen in the figure. Peak stresses are much closer to the GASC design value (800 MPa), with: $\sigma_{\mathrm{CS\_IM}} = 784$ MPa and $\sigma_{\mathrm{CS\_PL}} = 812$ MPa. The right panel shows the 3-D results for the PL. Peak stresses occur in local areas within the winding pack.
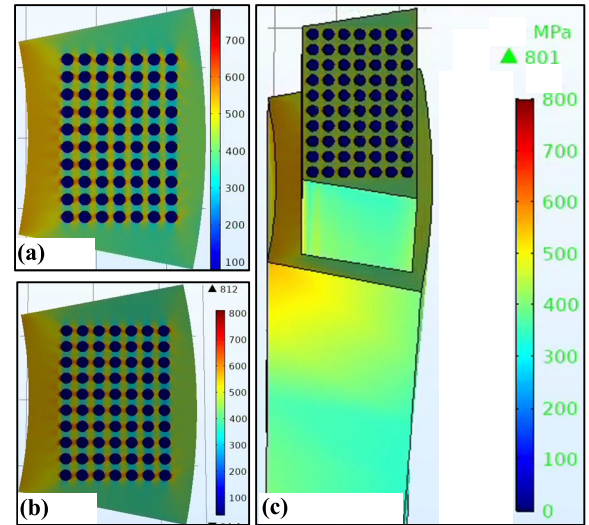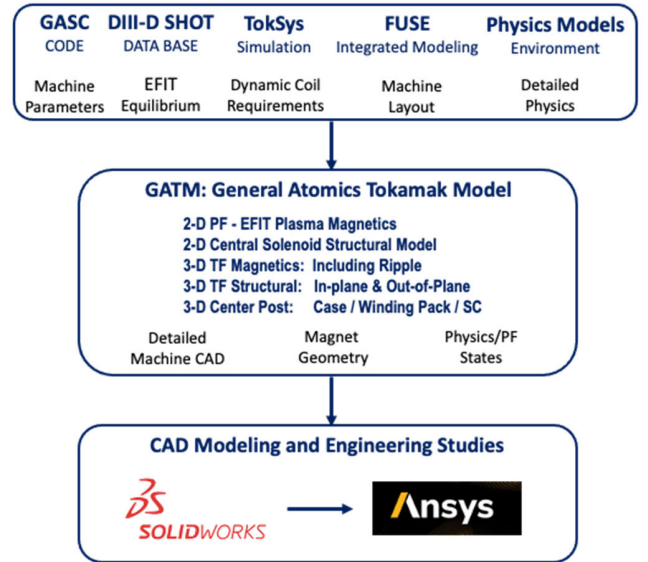
The full GATM 3-D model results reflect favorably on the GASC/FUSE analytic 2-D midplane CP stress model [5]. The GATM model provides added fidelity for the evaluation of the complex 3-D stress state produced by the full range of tokamak magnet and plasma parameters.

IV. GA TOKAMAK MODELING ENVIRONMENT

Over many years, GA has been developing an extensive set of tokamak modeling tools. Fig. 11 shows some of these tools and GATM's general relationship with these tools. Model input parameters are generated by a number of GA-related tools. In the current study, most information passed to GATM from GASC/FUSE, EFIT, and DIII-D shot database. The routines connecting this information to the GATM Comsol model are done manually by files through MATLAB and Excel programs as part of the GATM environment. Other connections are expected in future versions. The present GATM models and current states are being output to SolidWorks and Ansys for further structural refinement and validation of GATM results.

V. SUMMARY AND FUTURE PLANS

A general 3-D tokamak magnet modeling environment has been developed within the Comsol Multiphysics FE computational domain. It has been applied to DIII-D and potential future tokamaks. DIII-D results are comparable with the original design specification developed over 45 years ago. Applied to an FPP geometry, GATM provides needed detail for magnet component specification and partially validates the simpler 2-D models used in systems codes. GATM is interfaced with many GA physics and engineering models used for tokamak development and provides a basis for more detailed analysis using commercial engineering FE models. Future development is expected in both the model architecture as well as with interfaces to the evolving GA tokamak analysis environment. Specifically, its parameterized model can easily be applied to existing devices such as EAST, KSTAR, and ITER. The use of these devices would provide a connection to other studies for model validation and increased confidence for future device analysis.

APPENDIX A
GEOMETRIC MODELS

A. Tokamak Plasma Shape Type Geometric Model [14]

$$r = R_0 + a \cos[\theta + \delta \sin(\theta) - \xi \sin(2\theta)] \quad \text{(A1)}$$
$$z = \kappa a \sin[\theta + \xi \sin(2\theta)] \quad \text{(A2)}$$

where R_0 = Major-Radius, a = Minor-Radius, κ = Elongation, δ = Triangularity, and ξ = Squareness. θ is an angular parameter similar to a poloidal angle. This parameterization is available for use in plasma shape, TF, and PF boundaries.

B. Double-Ellipse Geometrical Model

$$r_i = R_i + a_i \cos(\theta) \quad \text{(A3)}$$
$$z_i = Z_i + b_i \sin(\theta) \quad \text{(A4)}$$

where the subscript $i = 1, 2$ refers to the inner and outer ellipses of the contours, respectively. $R_i, Z_i a_i b_i$ correspond to the usual description for an ellipse. This geometric prescription is currently only used for the TF centerline and boundaries.

All the above parameters are linked to allow minimal parameter manipulation to generate a full tokamak plasma/magnet geometry. In the typical system study, analysis input variables are: 1) Plasma: $R_{0p} a_p \kappa_p \delta_p \xi_p = 0$ and 2) TF: $R_{CP}, Z_{CP}, R_{TF}, R_{TF\_leg}, \Delta R_{CP}$, and ΔR_{TF}. Many of these inputs are generated by the GASC and input into the GATM environment. GASC provides essential information on the CS geometry: $\Delta R_{CS}, \Delta R_{CP\_CS}$. Outer PF coils are mapped from the outer contours of the TF coil using the plasma-based formulas above. Much of this architecture is duplicated in MATLAB and Excel for generation and model checking.

APPENDIX B
MAPPING DIII-D SHOT TO GATM

DIII-D shot database [8] contains a wide range of tokamak-relevant operational data and is valuable for characterizing NGT devices. In the present study, a particular shot is analyzed for flux utilization during DIII-D plasma ramp-up, and its properties are used to scale the equilibrium to the target GATM parameters. The following steps are taken in the mapping.
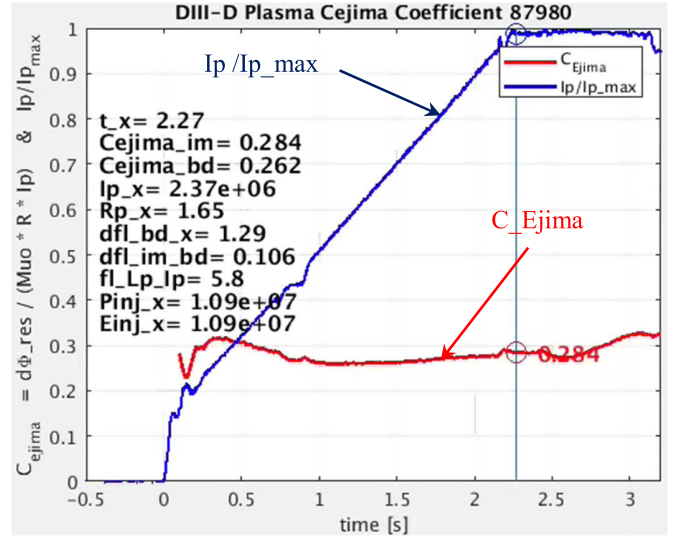

Fig. 12. Ejima et al. [11] coeficient ramp-up time evolution of target DIII-D shot S87980. $C_{\text{Ejima\_im}} = 0.28$ (IM to PL states) and is one of the best values achieved in DIII-D. Other parameters reflect other plasma ramp-up factors including $Einj\_x \sim 11$ GJ of auxiliary injected energy, which is important for achieving low C_{Ejima}.

A. DIII-D Shot Flux Partitioning

Flux partitioning during plasma ramp is best characterized using Ejima's formulation developed early in the Doublet III operations [11]. Flux components inductive (Φ_I) and resistive (Φ_R) are determined between the Initial Magnetization (IM) state, i.e., $t = 0$, and the current flattop state [PLasma (PL)]. The model determines the inductive and resistive flux provided by the PF coil system. The inductive flux requirement is intrinsically included in the EFIT equilibrium. The resistive part is contained in the dimensionless Ejima coefficient (C_{Ejima}) [11]

$$C_{\text{Ejima}} = \frac{\Delta \Phi_R}{\mu_0 R_0 I_p}; \quad \Delta \Phi_R = \int I_p \mathfrak{R}_p dt$$
$$\mathfrak{R}_p = \frac{\int 2\pi \rho J_p^2 R_p dA}{\left(\int J_p dA\right)^2}. \quad \text{(A5)}$$

Analysis of the target DIII-D discharge using this procedure is shown in Fig. 12. The IM to PL coefficient $C_{\text{Ejima\_im}} = 0.28$ is one of the best observed in DIII-D.

B. Mapping to GATM

DIII-D equilibrium is mapped to the GATM environment by scaling the plasma current states to the appropriate GATM size using R_0 for the scaling. In this FPP analysis, we use $C_{\text{Ejima\_FPP}} = 0.35$ as a conservative value for design. Representative GATM PF current states are determined using a single value decomposition (SVD) requiring constant flux on the plasma separatrix. Comparing shapes in Fig. 7(b) and (c) shows the similarity in flux shape between the DIII-D and GATM shapes. Other experiments or model-based equilibrium can easily be loaded into any of the GATM states using the above formulation and interfaces.

REFERENCES

[1] J. L. Luxon, "A design retrospective of the DIII-D tokamak," *Nucl. Fusion*, vol. 42, no. 5, pp. 614–633, May 2002, doi: 10.1088/0029-5515/42/5/313.

[2] D. B. Weisberg et al., "An integrated design study for an advanced tokamak to close physics gaps in energy confinement and power exhaust," *Fusion Sci. Technol.*, vol. 79, no. 3, pp. 320–344, Apr. 2023, doi: 10.1080/15361055.2022.2149210.

[3] R. J. Buttery et al., "The advanced tokamak path to a compact net electric fusion pilot plant," *Nucl. Fusion*, vol. 61, no. 4, Apr. 2021, Art. no. 046028, doi: 10.1088/1741-4326/abe4af.

[4] *COMSOL Multiphysics V. 6.1.* COMSOL AB, Stockholm, Sweden. Accessed: 2022. [Online]. Available: https://www.comsol.com/

[5] R. D. Stambaugh et al., "Fusion nuclear science facility candidates," *Fusion Sci. Technol.*, vol. 59, no. 2, pp. 279–307, Feb. 2011, doi: 10.13182/fst59-279.

[6] J. A. Leuer et al., "DIII-D integrated plasma control tools applied to next generation tokamaks," *Fusion Eng. Des.*, vol. 74, nos. 1–4, pp. 645–649, Nov. 2005, doi: 10.1016/j.fusengdes.2005.06.256.

[7] L. L. Lao, H. S. John, R. D. Stambaugh, and W. Pfeiffer, "Separation of β_p and ℓ_i in tokamaks of non-circular cross-section," *Nucl. Fusion*, vol. 25, no. 10, pp. 1421–1436, Oct. 1985, doi: 10.1088/0029-5515/25/10/004.

[8] B. G. Penaflor, D. A. Piglowski, R. D. Johnson, and B. B. McHarg, "Custom open source solutions for DIII-D data acquisition and control systems," in *Proc. 8th IAEA Tech. Committee Meeting Control Data Acquisition Remote Participation For Fusion Res.*, Livermore, CA, USA, 2011, pp. 1977–1980, doi: 10.1016/j.fusengdes.2012.07.011.

[9] *ITER Design Description Document*, document DDD-11, Magnets-Design Basis, 22HVG6_v1_4, Sep. 2009.

[10] V. S. Mukhovatov and V. D. Shafranov, "Plasma equilibrium in a tokamak," *Nucl. Fusion*, vol. 11, p. 605, Dec. 1971, doi: 10.1088/0029-5515/11/6/005.

[11] S. Ejima, R. W. Callis, J. L. Luxon, R. D. Stambaugh, T. S. Taylor, and J. C. Wesley, "Volt-second analysis and consumption in doublet III plasmas," *Nucl. Fusion*, vol. 22, no. 10, pp. 1313–1319, Oct. 1982, doi: 10.1088/0029-5515/22/10/006.

[12] J. A. Leuer et al., "Tokamak start-up modeling and design for EAST first plasma campaign," *Fusion Sci. Technol.*, vol. 57, no. 1, pp. 48–65, Jan. 2010, doi: 10.13182/fst10-a9268.

[13] J. A. Leuer et al., "Plasma startup design of fully superconducting tokamaks EAST and KSTAR with implications for ITER," *IEEE Trans. Plasma Sci.*, vol. 38, no. 3, pp. 333–340, Mar. 2010, doi: 10.1109/TPS.2009.2037890.

[14] O. Sauter, "Geometric formulas for system codes including the effect of negative triangularity," *Fusion Eng. Des.*, vol. 112, pp. 633–645, Nov. 2016, doi: 10.1016/j.fusengdes.2016.04.033.

[15] Doublet III Fusion Staff, *Doublet III Design*, GA-A-13318, General Atomics Co, San Diego, CA, USA, Jan. 1975, doi: 10.2172/5041107.

[16] E. E. Reis et. al., "Stress analysis of doublet III toroidal coil," in *Proc. IEEE 6th Symp. Eng. Prob. Fusion Res.*, Mar. 1975, pp. 618–622, doi: 10.2172/4093377.

[17] E. L. Wilson, K. J. Bathe, F. E. Peterson, and H. H. Dovey, "SAP—A structural analysis program for static linear systems," *Nuc. Eng. Des.*, vol. 25, no. 2, pp. 257–274, 1973, doi: 10.1016/0029-5493(73)90048-4.

[18] E. E. Reis, "Modifications to TF coils for DIII-D," in *Proc. 11th Symp. Fusion Eng.*, Austin, TX, USA, 1985, pp. 271–278.

[19] E. E. Reis and E. Chin, "Structural response of the DIII-D toroidal field coil to increased lateral loads," in *Proc. 20th IEEE/NPSS Symp. onFusion Eng.*, San Diego, CA, USA, Oct. 2003, pp. 577–580, doi: 10.1109/FUSION.2003.1426713.

[20] E. E. Reis, R. A. Sweig, and P. W. Trester, "Determination of a permissible size flaw in the doublet III toroidal field coil," in *Proc. 8th Symp. Eng. Problems Fusion Res.*, San Francisco, CA, USA, 1979, pp. 98–102.

[21] *ASME Boiler & Pressure Vessel Code*. New York, NY, USA: American Society of Mechanical Engineers, 2021.

[22] L. G. Davis and F. A. Puhn, "Doublet 111 anti-torque structure," in *Proc. 6th Symp. Eng. Problems Fusion Res.*, San Diego, CA, USA, 1975, pp. 635–639. [Online]. Available: https://www.osti.gov/servlets/purl/4132934

[23] J. A. Leuer and J. C. Wesley, "ITER plasma start-up modeling," in *Proc. 15th IEEE/NPSS Symp. Fusion Eng.*, Oct. 1993, pp. 629–633, doi: 10.1109/FUSION.1993.518409.

[24] J. File, R. G. Mills, and G. V. Sheffield, "Large superconducting magnet designs for fusion reactors," *IEEE Trans. Nucl. Sci.*, vol. NS-18, no. 4, pp. 277–282, Aug. 1971, doi: 10.1109/TNS.1971.4326354.

James A. Leuer (Member, IEEE) received the B.S. degree in aerospace engineering from San Diego State University, San Diego, CA, USA, in 1971, and the M.S. degree in engineering physics from the University of California at San Diego, San Diego, in 1972.

He is a semi-retired, Scientist/Engineer at General Atomics (GA), San Diego. He is in the Energy Division and has over 40 years of experience in the analysis of magnetic fusion tokamak machines and experiments. As a team member of the DIII-D National Fusion Facility Program, he has developed numerous codes for detailed analysis of tokamak fusion devices. He was one of the initial developers of the GA TokSys environment, which allows for integrated dynamic simulation of major tokamak systems and which was used in startup scenarios development of KSTAR and EAST tokamaks. He is the original author of the GA System Code (GASC), which is being used for the analysis of next-generation tokamaks. At several other organizations, including the Naval Underwater Research and Development Center, Science Applications Inc., and Nuclear Energy System Company, he has worked in many scientific areas including nuclear power generation, nuclear effects modeling, electromagnetic component design, combustion research, compressor design, hydrodynamic and turbulence modeling, and other general energy-related phenomena. He has developed numerous codes including models for tokamak plasma equilibrium, Electromagnetic Launch Systems (EMALS), Magnetic Resonance Imaging (MRI) magnets, Inertial Confinement Fusion (ICF) magnets, superconducting gyrotron magnets, High-Temperature Gas Cooled Reactors (HTGR), 3-D dynamic particle trajectory simulations, Linear Induction Motors (LIM), Superconducting Magnetic Energy Storage (SMES), ocean wave energy extraction, and rail gun performance evaluation. He has authored two U.S. patents.

Mr. Leuer is a member of the American Physical Society and a CA Registered Professional Engineer. He received the 1970 San Diego State Outstanding Aerospace Engineering Award, the 2009 Innovative Experimental Science, DOE/DIII-D-Tokil Jensen Award, and the 2012 Chinese Academy of Science Visiting Professorship Scholarship.

D. Weisberg, photograph and biography are not available at the time of publication.

R. MacDonald, photograph and biography are not available at the time of publication.

I. Favela received the B.S. degree from the California State Polytechnic University, Pomona, CA, USA, in 2010. He is currently pursuing the M.S. degree in mechanical engineering with a focus on multiscale mechanical modeling at San Diego State University, San Diego, CA, USA.

He is currently a Mechanical Engineer with General Atomics in the DIII-D fusion energy program. He leads projects in the design and development of new plasma-facing armor and machine integration of DIII-D in support of new plasma physics projects. His recent work relates to component evaluation via ANSYS and other FEA models. He is performing eddy current analysis of off-normal plasma events like disruptions to verify the structural integrity of internal DIII-D components.

Mr. Favela was awarded a patent for the design of a solid-state relay during his time at Sensata Technologies in 2017.

Paul Beharrell received the master's degree (Hons.) in superconductivity and cryogenics and the Ph.D. degree in applied superconductivity from the University of Southampton, Southampton, U.K., in 1994 and 2000, respectively.

Since 2019, he has been a Principal Scientist/Engineer at the General Atomics Magnet Technologies Center, part of General Atomics' Energy Group. He is engaged in a wide range of technologies across the Energy Group, including High-Temperature Superconducting (HTS) magnets, nuclear fusion devices, particle accelerators, and novel applications in the fields of space, diagnostics, and exotic propulsion systems. Well-versed in numerous engineering and physics disciplines, system integration, manufacturing engineering, and multiphysics computational analysis, he is highly experienced in technical design, from initial concepts to fully realized production. He has been involved with innovation and application development in the fields of superconducting magnet systems, cryogenic engineering, scientific instrumentation, and emerging energy technologies for almost 30 years. He has been responsible for many innovations and new products. While operating his own company in China, in 2005, he designed and constructed the first commercial-scale superconducting magnetic separation system incorporating a conduction-cooled magnet system. This was also the first large-scale superconducting magnet constructed in the country. Continuing with the development of specialized electromagnetic and cryogenic systems, he moved to the USA in 2009 to establish the in-house manufacture of superconductive components for a market leader in instrumentation systems.

Dr. Behrrell was nominated for the 2014 Carl H. Rosner Award for Entrepreneurship in Superconductivity.

D. Appelt, photograph and biography are not available at the time of publication.

R. Buttery, photograph and biography are not available at the time of publication.

C. Crowe, photograph and biography are not available at the time of publication.

N. Eidietis, photograph and biography are not available at the time of publication.

B. Grierson, photograph and biography are not available at the time of publication.

L. Holland, photograph and biography are not available at the time of publication.

K. Holtrop received the B.S. degree in engineering physics from the University of Colorado, Boulder, CO, USA, in 1989, and the M.S. degree in materials science from the University of California at San Diego, San Diego, CA, USA, in 1997.

He is currently the Deputy Director of Machine Operations for the DIII-D National Fusion Facility in San Diego. He assists in leading a large multi-skilled, multi-institutional team of 80 personnel in maintaining and running the device with a focus on flexibility, efficiency, and safety while maintaining operational reliability. In addition, he assists in implementing major facility upgrades of the Tokamak Operation and Mechanical Systems.

A. Kellman, photograph and biography are not available at the time of publication.

James L. Luxon received the Ph.D. degree in atomic physics from the University of Michigan, Ann Arbor, MI, USA, in 1972.

He retired from General Atomics (GA) in 2005 and was the Director of the DIII-D National Fusion Facility in San Diego, CA, USA, from 1991 to 2002. He is still providing guidance and support to the DIII-D program as a retired director. He has been involved in many of the GA's fusion programs including Doublet II-A, Doublet III, and DIII-D. He was at the University of Michigan, from 1972 to 1974.

C. Murphy, photograph and biography are not available at the time of publication.

Z. Piec, photograph and biography are not available at the time of publication.

G. Sips (Member, IEEE), photograph and biography are not available at the time of publication.

M. Van Zeeland, photograph and biography are not available at the time of publication.

Amani Zalzali received the B.S. and M.S. degrees in physics from the American University of Beirut, Beirut, Lebanon, in 2011 and 2014, respectively, the M.Phil. degree in engineering from the University of Cambridge, Cambridge, U.K., in 2017, and the Ph.D. degree in computational plasma physics from the University of Warwick, Coventry, U.K., in 2022.

She is currently a Strategic Development Associate at the energy group at General Atomics in San Diego, CA, USA, working on creating business partnerships in the fusion industry to develop a roadmap for enabling technologies that are necessary for commercializing fusion energy. Before this role, she worked on the design of an advanced tokamak for use in a demonstration fusion pilot plant.

Dr. Zalzali is a member of Women in Fusion (WiF) and served as a Physics Ambassador at the Institute of Physics (IOP) in the U.K.